

Performance Improvement and Energy Cost Reduction under Different Scenarios for a Parabolic Trough Solar Power Plant in the Middle-East Region

Authors:

Mujeeb Iqbal Soomro, Abdullah Mengal, Qadir Nawaz Shafiq, Syed Aziz Ur Rehman, Shakir Ali Soomro, Khanji Harijan

Date Submitted: 2019-09-13

Keywords: Abu Dhabi, levelized cost of energy, performance improvement, System Advisor Model, concentrated solar power

Abstract:

Concentrated solar power (CSP) is a leading renewable energy technology, and the parabolic trough (PT) is one of the most used configurations of CSP. In the present study, the performance improvement and energy cost reduction of a 50 MWe PT plant for Abu Dhabi, United Arab Emirates (UAE) is presented. The simulations were carried out using the System Advisor Model software. The analyses of a PT plant with different technologies/parameters are undertaken in the first instance for seven cases. These cases include solar multiple, solar collectors, receivers, heat transfer fluid, cooling system (evaporative and air-cooled), thermal energy storage system (4?12 h), and fossil dispatch mode (0.25 to 1.0). Based on these analysis, the eighth case, which is found to be the best-case scenario in this study, was considered by taking into account the best of preceding case results and was determined to be the most suitable both in terms of performance and cost reduction. It is, therefore, concluded from this study that the utilization of CSP plants with a proper selection of technology could help reduce energy costs and environmental pollution, enhance system performance, and meet energy demands effectively.

Record Type: Published Article

Submitted To: LAPSE (Living Archive for Process Systems Engineering)

Citation (overall record, always the latest version):

LAPSE:2019.1008

Citation (this specific file, latest version):

LAPSE:2019.1008-1

Citation (this specific file, this version):


LAPSE:2019.1008-1v1

DOI of Published Version: <https://doi.org/10.3390/pr7070429>

License: Creative Commons Attribution 4.0 International (CC BY 4.0)

Article

Performance Improvement and Energy Cost Reduction under Different Scenarios for a Parabolic Trough Solar Power Plant in the Middle-East Region

Mujeeb Iqbal Soomro ^{1,*}, Abdullah Mengal ², Qadir Nawaz Shafiq ¹, Syed Aziz Ur Rehman ³, Shakir Ali Soomro ⁴ and Khanji Harijan ⁵

¹ Department of Mechanical Engineering, Mehran University of Engineering & Technology, SZAB Campus, Khairpur Mir's 66020, Sindh, Pakistan

² Department of Mechanical Engineering, Balochistan University of Engineering and Technology, Khuzdar 89100, Balochistan, Pakistan

³ Department of Environmental Sciences, University of Veterinary and Animal Sciences, Lahore 54000, Pakistan

⁴ Department of Electrical Engineering, Mehran University of Engineering & Technology, SZAB Campus, Khairpur Mir's 66020, Sindh, Pakistan

⁵ Department of Mechanical, Mehran University of Engineering & Technology, Jamshoro 76062, Sindh, Pakistan

* Correspondence: mujeebsoomro@muetkhp.edu.pk

Received: 11 June 2019; Accepted: 30 June 2019; Published: 5 July 2019



Abstract: Concentrated solar power (CSP) is a leading renewable energy technology, and the parabolic trough (PT) is one of the most used configurations of CSP. In the present study, the performance improvement and energy cost reduction of a 50 MWe PT plant for Abu Dhabi, United Arab Emirates (UAE) is presented. The simulations were carried out using the System Advisor Model software. The analyses of a PT plant with different technologies/parameters are undertaken in the first instance for seven cases. These cases include solar multiple, solar collectors, receivers, heat transfer fluid, cooling system (evaporative and air-cooled), thermal energy storage system (4–12 h), and fossil dispatch mode (0.25 to 1.0). Based on these analysis, the eighth case, which is found to be the best-case scenario in this study, was considered by taking into account the best of preceding case results and was determined to be the most suitable both in terms of performance and cost reduction. It is, therefore, concluded from this study that the utilization of CSP plants with a proper selection of technology could help reduce energy costs and environmental pollution, enhance system performance, and meet energy demands effectively.

Keywords: concentrated solar power; System Advisor Model; performance improvement; leveled cost of energy; Abu Dhabi

1. Introduction

Conventional sources of energy production are depleting, and their adverse effects on the environment, such as climate change and global warming, are well known. Therefore, the utilization of renewable energy for energy production is increasing in interest worldwide because of sustainable development and environmental concerns [1,2]. Renewable energy is a source of energy that can be naturally replenished and whose emissions are significantly lower than conventional energy sources [3]. Renewable energy sources (RES) are inexhaustible and widely spread on the earth's surface [4,5]. There has been a considerable increase in the utilization of RES in the last decade. It is reported that RES supplied 23.7% of the world's global electricity in 2015 [6].

RES include hydro, wind, biomass, geothermal, solar energy, and other sources. However, solar energy is the principal source of renewable energy because of its abundant availability. It is also more environmentally friendly compared to other RES [3,7]. A tremendous amount of energy, nearly 4000 trillion kWh per day, is provided by the sun, which is much higher than the current energy supplied by tidal, nuclear, and fossil fuels [4,8]. The Direct Normal Insolation (DNI) is variable according to the geographic area, due to its stochastic character [9,10]. Two leading technologies for harvesting solar energy are solar photovoltaic (SPV) technology and concentrated solar power (CSP). SPV exploits solar energy to directly convert it into electricity, whereas CSP concentrates the sunlight onto a specific area to heat a working fluid for a process. The SPV is an advanced technology, and the capital and Levelized Cost of Energy (LCOE) is lower, which makes SPV a preferred option. However, energy storage is a critical issue in SPV [11]. Conversely, the share of CSP is growing for many reasons, which include (i) a relatively inexpensive thermal energy storage (TES) system; (ii) relatively higher efficiency; and (iii) relatively higher capacity factor [11].

CSP is one of the leading energy production technology. It utilizes concentrators/reflectors to concentrate sunlight to heat a working fluid. The heated working fluid can be used in a process industry/to convert water into steam for a Rankine cycle. The most commonly used application of CSP is electricity generation. However, CSP can be also used for other heat applications [12]. A schematic diagram for the principle operation of the CSP plant, for electricity production, is presented in Figure 1. For sustainability, a TES system is used to store additional thermal energy, which can be utilized in the unavailability of sunlight. Four widely recognized CSP technologies include parabolic trough collectors (PTCs), linear Fresnel reflectors (LFRs), solar power towers (SPTs), and parabolic dish collectors (PDCs), as shown in Figure 2 [6,13]. Further, the PTCs and LFRs are categorized as line focused, whereas the SPTs and PDCs are categorized as point focused [14]. It is important to note that the PTC is the most mature and widely used CSP technology [14]. For a technology overview, a comparison of different CSP technologies is summarized in Table 1. The commercialization of CSP has increased progressively due to its advantages, such as higher efficiency, low operational cost, and being carbon-free. Renewable Energy Policy Network (REN21) reported that the total installed capacity of CSP increased up to 4.7 GW in 2015 [6]. The major stakeholders in installed CSP capacity were Spain and the United States, with 2.3 GW and 1.73 GW, respectively, as shown in Figure 3 [6]. The performance and energy cost of a CSP plant are critically affected by several components, such as collectors, receivers, heat transfer fluids (HTF), and the TES system. Therefore, to make CSP more competitive with other technologies, researchers focus on different efficiency improvements and cost reduction methods. These methods include a selection of appropriate technologies/components, technological breakouts/innovations, and the local manufacturing of components to be used in a CSP plant [15].

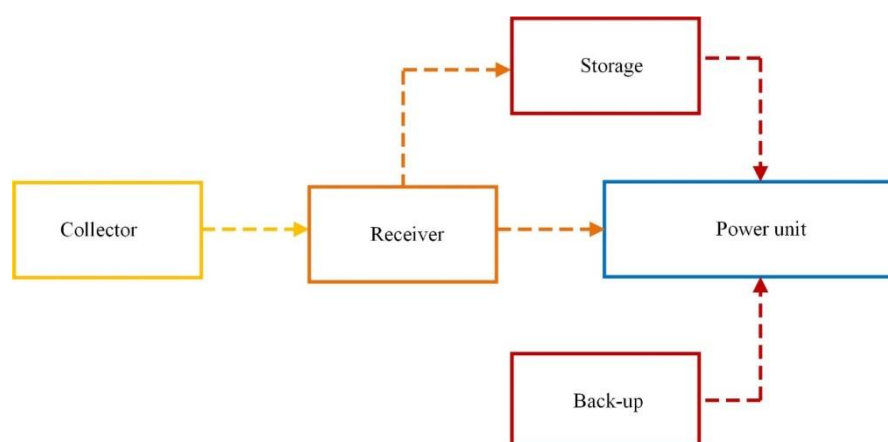


Figure 1. Principle operation of a concentrated Solar Power (CSP) plant.

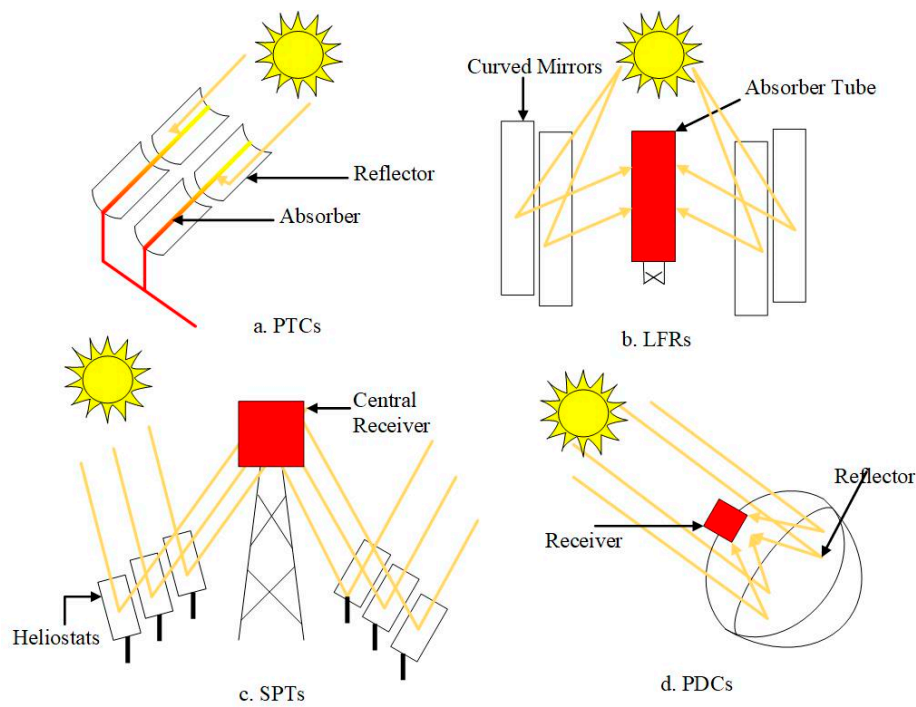


Figure 2. Types of CSP. Parabolic trough collectors (PTCs); linear Fresnel reflectors (LFRs); solar power towers (SPTs); parabolic dish collectors (PDCs).

Table 1. A comparison of different CSP technologies. Adapted from [16,17].

	Relative Cost	Land Occupancy	Cooling Water (L/MWh)	Thermo-Dynamic Efficiency	Operating Temperature Range (°C)	Solar Concentration Ratio	Outlook for Improvements
PTCs	Low	Large	3000 or dry	Low	20–400	15–45	Limited
LFRs	Very low	Medium	3000 or dry	Low	50–300	10–40	Significant
SPTs	High	Medium	1500 or dry	High	300–565	150–1500	Very significant
PDCs	Very high	Small	None	High	120–1500	100–1000	High potential through mass production

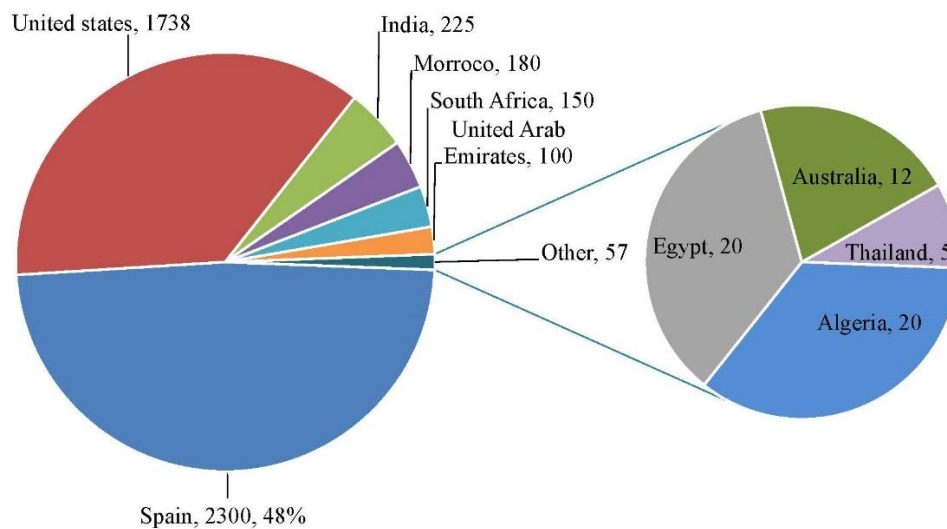


Figure 3. CSP global capacity in MW by the end of 2015.

Several studies [18–21] have reported that the performance of CSP technology can be increased, and, consequently, the cost of energy can be reduced. The measures that contribute towards these goals include technological advancements and the appropriate selection of concentrators, absorbers, heat transfer fluids, and backup systems. Kearney et al. [18] assessed utilizing molten salt (solar salt and Hitec XL) instead of synthetic oil as an HTF for performance improvement and cost reduction. The results revealed that the performance could be considerably increased and the levelized cost of energy (LCOE) could be reduced simultaneously by using molten salts as HTF. Giostri et al. [19] presented a performance comparison and annual energy production of parabolic trough (PT) plants based on synthetic oil and solar salt as HTFs. The results revealed that efficiency improved up to 6% when solar salt was used as an HTF instead of synthetic oil. Wagner et al. [20] presented performance and cost analysis of a 110 MW PT CSP plant with a TES system, a natural gas-fired system, both with and without backup systems. Kassem et al. [21] presented a techno-economic analysis of a few CSP technologies, including PT, SPT, and LFR for Riyadh, Kingdom of Saudi Arabia (KSA). The authors considered six power plant scenarios with different conditions, which include CSP plants without storage, with storage (3 h–12 h), and dry cooling. The simulations were carried out using the System Advisor Model (SAM) Software (National Renewable Energy Laboratory, 901 D. Street, S.W. Suite 930 Washington, D.C. 20024-2157, USA).

In this study, an attempt has been made to investigate the effects of different solar multiples, collectors, receivers, HTFs, cooling systems, TES systems, and fossil fuel backup systems for the performance improvement and cost reduction of a CSP system. Finally, performance and LCOE based on the best suitable case/condition were evaluated. A 50 MWe PT plant based on the Rankine cycle has been considered for the evaluation. The weather conditions of Abu Dhabi, United Arab Emirates (UAE) were incorporated for the analysis. The simulations for all cases were carried out using the SAM software. The performance results were reported in terms of annual energy production, gross-to-net conversion factor, and capacity factor, whereas economic evaluation has been reported in LCOE. The environmental and economic benefits of CSP plants in terms of the Clean Development Mechanism (CDM) under the Kyoto Protocol (KP) have also been analyzed to elaborate the environmental and financial feasibility of CSP plants.

The remainder of this paper is comprised of the methodology presented in Section 2, the results and discussion in Section 3. The conclusions drawn from this study are summarized in Section 4.

2. Methodology

2.1. System Description

The proposed 50 MWe PT plant mainly consists of three units. A visual representation of the PT plant is presented in Figure 4. The first unit is the PT solar field, which consists of parabolic shaped reflectors, absorber tubes, and solar field piping. The sunlight is incident on the parabolic reflector, which is concentrated onto a focal point on the absorber tube. An HTF is circulated in the absorber tubes to absorb the thermal energy. Then, the HTF is pumped into the second unit, i.e., the thermal storage unit. The thermal storage unit consists of two tanks named as hot storage tanks and cold storage tanks. It is important to note that the two storage tank is the most commonly used technique in commercial CSP plants [22]. The HTF flow forms hot storage tank to cold storage tank via steam generator where HTF exchanges the heat. The thermal storage serves two purposes: for storing additional thermal energy, if any, and supplying heat to the run the third unit, i.e., the power unit. The power unit, which is based on the Rankine cycle, consists of a steam generator, condenser, turbine, generator, and cooling tower. The heat is transferred from the HTF to the water in the steam generator to produce steam. The HTF, after transferring heat in the steam generator, flows to the thermal storage tank. The steam is expanded in the turbine and subsequently condensed in the condenser. The condensed water is cooled down in cooling tower so that it can be resupplied to the steam generator. The turbine is coupled with an electric generator to produce electricity.

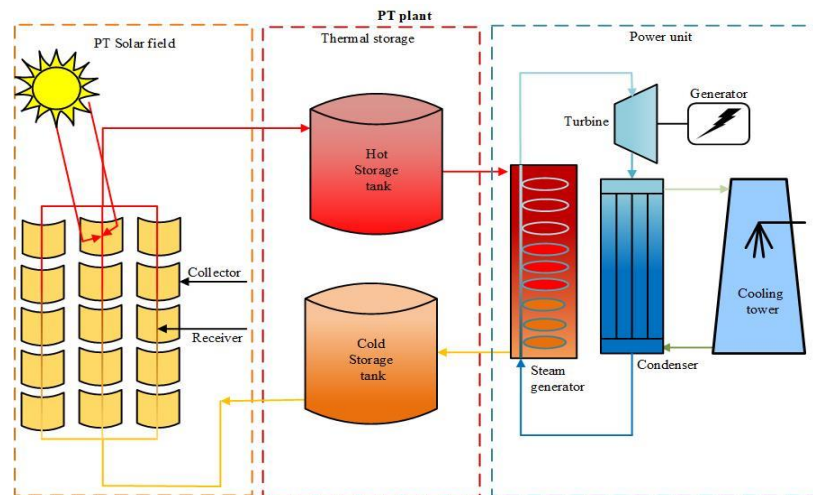


Figure 4. Schematic diagram of a parabolic trough (PT) plant.

2.2. PT Plant Analysis

The PT plant performance and cost analysis were conducted with the SAM software. SAM is an open-access software developed by the United States National Renewable Energy Laboratory [23]. SAM can be used for electricity generation systems for residential, commercial, and utility-scale projects [23]. Different RES, including solar, biomass, wind, and geothermal, can be modeled and simulated using the SAM software. Several studies on CSP have been carried using the SAM software [20,21,24].

In the present study, PT plant analysis was carried out for Abu Dhabi, UAE, because a good potential of solar energy is available in the country, as depicted in Figure 5 [25]. Further, the CSP market is also expanding in the region. The Direct Normal Insolation (DNI) reaches up to 6290 Wh/m²/day [26]. The hourly and monthly DNI for the selected region is depicted in Figures 6 and 7, respectively. It can be observed in Figure 6 that during the peak hours, the maximum DNI is 867.5 W/m² in September. However, the minimum DNI for the proposed location is 670.64 W/m² in December. For monthly data, it can be observed that the maximum and minimum DNI are 6847.261 W/m² and 5276.038 W/m² in May and December, respectively, as shown in Figure 7. The weather data for a typical meteorological year (TMY), which consists of direct normal insolation, ambient temperature, sun angle, solar azimuth angle, and the atmospheric pressure of an entire year, for the proposed location in the simulation is provided by the SAM software in the comma-separated value (CSV) file format [27]. The simulations for the PT plant were carried out for different cases/conditions to analyze the performance and LCOE. For the purpose of the investigation, a total of eight cases were considered, which include:

- Case 1. 50 MWe PT plant with different values of the solar multiple
- Case 2. 50 MWe PT plant with different collectors/solar collector assemblies (SCAs)
- Case 3. 50 MWe PT plant with different receivers/heat collection elements (HCEs)
- Case 4. 50 MWe PT plant with a different HTF
- Case 5. 50 MWe PT plant with different TES systems (4 h–12 h)
- Case 6. 50 MWe PT plant with different types of cooling systems
- Case 7. 50 MWe PT plant with different fossil fill fractions
- Case 8. 50 MWe PT plant with suitable parameter/components

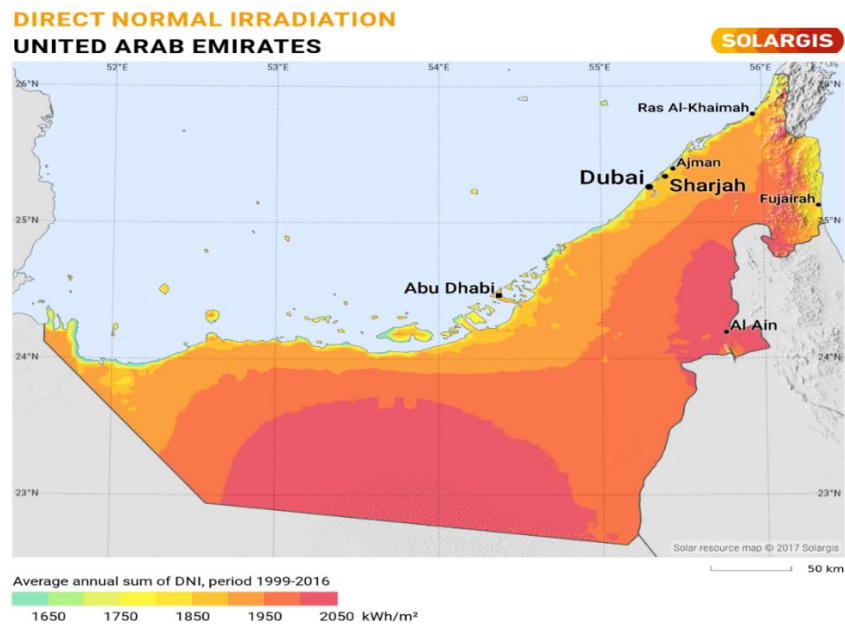


Figure 5. Solar map of the United Arab Emirates (UAE).

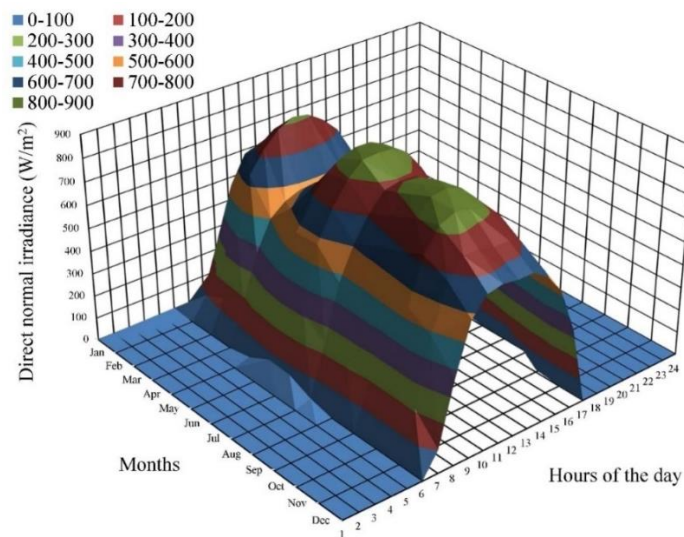


Figure 6. Hourly direct normal insolation (DNI) for UAE.

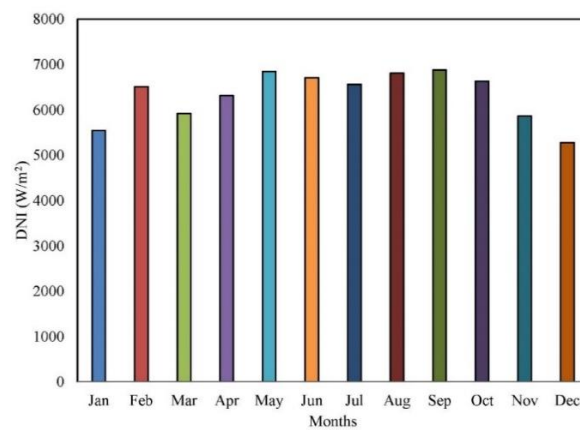


Figure 7. Monthly DNI for UAE.

The performance assessment of the proposed cases is presented in terms of annual energy production, the gross-to-net conversion factor, and the capacity factor. The gross-to-net conversion factor is defined as the ratio of net electric output to the gross electric output, whereas the capacity factor is defined as the ratio of predicted electrical output to the potential electrical output. Moreover, the cost assessment has been presented in terms of LCOE. LCOE is the current value of project costs expressed in cents per kilowatt-hour (¢/kWh) by the system in its life span. There are two types of LCOE, real LCOE and nominal LCOE. Real LCOE uses the constant dollar and inflation-adjusted values, whereas nominal LCOE uses current dollar values. It is important to mention that the real LCOE may be used for long term analysis, whereas nominal LCOE may be used for short term analysis [28]. The real LCOE and nominal LCOE can be calculated from Equation (1) and Equation (2), respectively:

$$LCOE_{(r)} = \frac{-C_o - \frac{\sum_{n=1}^N C_n}{(1-d_n)^n}}{\frac{\sum_{n=1}^N Q_n}{(1-d_r)^n}} \quad (1)$$

$$LCOE_{(n)} = \frac{-C_o - \frac{\sum_{n=1}^N C_n}{(1-d_n)^n}}{\frac{\sum_{n=1}^N Q_n}{(1-d_n)^n}} \quad (2)$$

where $LCOE_{(r)}$ = Real LCOE; $LCOE_{(n)}$ = Nominal LCOE; N = Investigation period; Q_n = Electricity produced in N years by the PT plant for the proposed location; C_o = Equity investment of the project; C_n = Annual cost of the project in N years; d_r = Real case discount rate; d_n = Nominal case discount rate (with inflation).

The equity investment cost is the amount of cash invested by the investor. It is defined as the difference between net capital cost and debt. The net capital cost is the total installed cost of the project. It includes the cost of the installation and operation of the proposed system [28]. The net capital cost is separated into three categories [28]:

- i. Direct capital cost: the cost of equipment and installation.
- ii. Indirect capital cost: sanctions, engineering, and land cost.
- iii. Operation and maintenance (O&M) cost: labor, equipment, and other costs associated with the operation and maintenance of the plant.

The general parameters/specifications used for the performance simulation and cost assessment of a 50 MWe PT plant for all the cases are listed in Table 2.

Table 2. General parameters/specification for the assessment of the proposed 50 MWe PT plant.

	Description	Specifications/Value
Location parameters	City	Abu Dhabi
	Country	UAE
	Longitude	54.65°E
	Latitude	24.43°N
Solar field parameters	Row spacing	15
	Stow angle	170°
	Deploy angle	10°
Power cycle	Design gross output	50 MWe
	Estimated gross-to-net conversion factor	0.9
	Estimated net output at design	45 MWe
	Rated cycle conversion efficiency	0.356
	Boiler operating pressure	100 bar
	Design loop outlet temperature	391 °C
	Design loop inlet temperature	293 °C
Financial parameters	Lifetime	25 years
	Inflation rate	2.5%/year
	Real discount rate	5.5%/year
	Nominal discount rate	8.14%/year

3. Results

The performance and cost assessment of a PT plant using different cases will be discussed in this section.

3.1. Case 1. A 50 MWe PT Plant with Different Values of the Solar Multiple

In the first case, the performance and cost assessment of the 50 MWe PT plant were carried out with different values of the solar multiple. The solar multiple represents the solar field aperture area as a multiple of the power cycle capacity. In designing of a CSP plant, determination of optimum solar field aperture area for a specified location is essential. Generally, an increase in the solar field areas increases the plant's electricity production and simultaneously reduces the LCOE. However, too large a solar field area will generate more thermal energy than the capacity of the TES system and power unit.

Moreover, an increase in the solar field areas increases the installation, operating, and maintenance cost. In general, a solar multiple of one ($SM = 1$) generates the thermal energy required to drive the power unit at its rated capacity without storage. However, a solar multiple greater than one ($SM > 1$) produces enough thermal energy to drive the power unit for more hours. Therefore, in the present study, to investigate the effect of the solar multiple on the performance and LCOE, the solar multiple varied from 1 to 5. The technical components/parameters that were used for the simulations are presented in Table 3. For this case, Euro Tough ET150 was selected as a collector because of its low cost, easy installation, and high optical efficiency [29]. Euro Tough ET150 is used in many CSP plants worldwide [21].

Table 3. Technical components/parameters for Cases 1 to 8. Heat transfer fluid (HTF); thermal energy.

Technical Parameters	Case 1	Case 2	Case 3	Case 4	Case 5	Case 6	Case 7	Case 8
Solar multiple	1–5	4	4	4	4	4	4	4
Collector	Euro Tough ET150	Different	Luz LS-3	Luz LS-3	Luz LS-3	Luz LS-3	Luz LS-3	Luz LS-3
Receiver	Schott PTR70	Schott PTR70	Different	Schott PTR70 2008	Schott PTR70 2008	Schott PTR70 2008	Schott PTR70 2008	Schott PTR70 2008
Condenser type	Evaporative	Evaporative	Evaporative	Evaporative	Evaporative	Evaporative/Air cooled	Evaporative	Evaporative
TES (h)	12	12	12	12	4–12	12	12	12
HTF	Therminol VP-1	Therminol VP-1	Therminol VP-1	Different	Therminol VP-1	Therminol VP-1	Therminol VP-1	Therminol VP-1
Fossil fill fraction	0	0	0	0	0	0	0.25–1.0	1.0

On the other hand, SchottPTR70 was selected as the receiver because it is the most commonly used in CSP plants [30], whereas Therminol VP-1 was selected as HTF for the simulations because it is also widely used in PT plants [30]. The results of the simulations for the present case are summarized in Table 4. It can be observed that with an increase in solar multiple from 1 to 4, the annual energy production, gross to net conversion factor, and capacity factor increased. However, LCOE reduced with an increase in the solar multiple from 1 to 4, although the capital cost of the PT plant increased with an increase in the solar multiple, but higher energy production leads to a reduction of the LCOE.

Table 4. Case 1. Results of simulations for a 50 MWe PT plant with different solar multiples. Levelized cost of energy (LCOE).

	Solar Multiple				
	1	2	3	4	5
Performance parameters					
Annual energy (GWh)	64.202	133.018	203.293	272.049	301.365
Gross-to-net conversion factor (%)	88.8	91.7	92.7	93.01	92.8
Capacity factor (%)	16.3	33.7	51.6	69.03	76.4
Financial parameters					
Net capital cost (\$)	312,909,120	418,891,968	524,874,816	634,512,256	846,478,016
Nominal LCOE (¢/kWh)	8.35	5.2	4.17	3.71	4.39
Real LCOE (¢/kWh)	6.57	4.09	3.28	2.92	3.45

Moreover, it can be observed that a further increase in the solar multiple, from 4 to 5, reduced the gross-to-net conversion factor and the capacity factor and considerably increased the LCOE. This result is attributed to the fact that a much higher solar multiple increased the thermal energy beyond the limits of both the TES system and the power block. Subsequently, a higher capital cost leads to an increased LCOE. Therefore, the optimum value (SM = 4) is obtained for the present case, and this value will be considered in further simulations.

3.2. Case 2. A 50 MWe PT Plant with Different Collectors/SCA

In the second case, the performance and cost assessment of the 50 MWe PT plant were carried out using different collectors/SCAs. The list of different commercially available collectors with specifications, which were used for the simulations, are presented in Appendix A. For this case, the technical components/parameters for the simulations are presented in Table 3, whereas the results of simulations are summarized in Table 5. It can be seen that considerable variations are found in the results. However, it can also be observed that the performance of the Luz LS-3 is higher in terms of its annual energy production (277.974 GWh) and capacity factor (70.5%). This result is attributed to the higher efficiency of the collector.

Moreover, the cost assessment revealed that the lowest LCOE is also obtained for Luz LS-3. The reason behind the lowest LCOE is higher energy production, which tends to reduce the LCOE. The simulations showed higher performance and the lowest LCOE for the Luz LS-3. Therefore, Luz LS-3 will be considered in further simulations in the present study.

3.3. Case 3. A 50 MWe PT Plant with Different Receivers/HCE

In the third case, the performance and cost assessment of a 50 MWe PT plant were carried out using different receivers/HCEs. The list of different commercially available receivers with specifications, which were used for the simulations, are presented in Appendix B. For this case, the technical components/parameters for the simulations are presented in Table 3. Luz LS-3 was selected as the SCA because of its higher performance and low LCOE (as discussed in case 2). The simulation results are summarized in Table 6. For the present case, it can be observed that the differences in the results are minimal. Therefore, a strong preference is not justifiable. It is worth noting that the results obtained from case 3 are in good agreement with the simulation results available in the literature [29]. However, generally, SchottPTR70 2008 is preferable because it is widely employed in CSP plants [30]. Therefore, SchottPTR70 2008 will be considered in further simulations in the present study.

Table 5. Case 2. Results of simulations for a 50 MWe PT plant with different collectors/SCAs.

	Collectors									
	Euro Tough ET150	Luz LS-2	Luz LS-3	Solargenix SGX-1	Albisa Trough AT150	Siemens Sunfield 6	SkyFuel SkyTrough (with an 80 mm OD Receiver)	FLABEG Ultimate Trough RP6 (with an 89 mm Outer Diameter) Receiver for Oil HTF)	FLABEG Ultimate Trough RP6 (with a 70 mm OD Receiver for Molten-Salt HTF)	
	Performance parameters									
Annual energy (GWh)	272.049	266.538	277.974	275.666	271.974	274.296	277.112	127.846	129.83	
Gross-to-net conversion factor (%)	93	95.7	94.7	95.2	93	94.5	94.1	90.3	90.4	
Capacity factor (%)	69	67.6	70.5	69.9	69	69.9	70.3	32.4	32.9	
	Financial parameters									
Net capital cost (\$)	634,512,256	636,094,720	632,075,904	635,317,184	634,483,328	636,917,184	642,866,560	616,900,672	624,560,448	
Nominal LCOE (¢/kWh)	3.71	3.8	3.62	3.67	3.71	3.7	3.69	7.7	7.67	
Real LCOE (¢/kWh)	2.92	2.99	2.85	2.89	2.92	2.91	2.9	6.05	6.03	

Table 6. Case 3: Results of simulations for a 50 MWe PT plant with different receivers/HCEs.

	Receivers							
	Schott PTR70	Schott PTR70 2008	Solel Universal Vacuum Air Collector (UVAC) 3	Siemens UVAC 2010	Schott PTR80	Royal Tech CSP RTUVR 2014 (Manufacturer Specifications)	Royal Tech CSP RTUVR 70M4 (Manufacturer Specifications)	TRX70-125 (Manufacturer Specifications)
	Performance parameters							
Annual energy (GWh)	277.974	288.502	289.183	287.23	288.119	290.237	290.382	289.002
Gross-to-net conversion factor (%)	94.7	94.8	94.8	94.7	95.6	94.9	94.8	94.8
Capacity factor (%)	70.5	73.2	73.4	72.9	73.1	73.6	73.7	73.3
	Financial parameters							
Net capital cost (\$)	417,673,760	417,673,760	415,237,408	412,801,024	422,546,592	422,546,592	420,110,176	417,673,760
Nominal LCOE (¢/kWh)	632,075,904	629,639,552	627,203,136	622,330,368	641,821,440	639,385,024	636,948,672	632,075,904
Real LCOE (¢/kWh)	3.62	3.48	3.46	3.45	3.54	3.5	3.49	3.48

3.4. Case 4. A 50 MWe PT Plant with Different HTF

In the fourth case, the performance and cost assessment of the 50 MWe PT plant were carried out using different HTF. The list of different commercially available HTFs with specifications, which were used for the simulations, are presented in Appendix C. The technical components/parameters for the simulations for the current case are listed in Table 3. The Luz LS-3 was selected as the SCA because of its higher performance and low LCOE (Case 2), whereas the Schott PTR70 2008 was selected based on the Case 3 results. The results of the simulations are summarized in Table 7. In the present case, it can be observed that the performance of Therminol VP-1 is the highest in terms of annual energy production (288.502 GWh), the gross-to-net conversion factor (94.8%), and capacity factor (73.2%). This result is attributed to its higher storage exergetic efficiency.

Moreover, cost assessment revealed that the lowest $LCOE_{(n)}$ (3.48 ¢/kWh) and $LCOE_{(t)}$ (2.73 ¢/kWh) was also obtained for Therminol VP-1. The reason behind this low LCOE is higher energy production, which tends to reduce the LCOE. This could be the reason that the Therminol VP-1 has been widely deployed in PT plants worldwide [30]. Since the simulations revealed higher performance and the lowest LCOE with Therminol VP-1, it will be considered as the HTF in further simulations in the present study.

3.5. Case 5. A 50 MWe PT Plant with Different TES System (4 h–12 h)

In the fifth case, the performance and cost assessment of the 50 MWe PT plant were carried out using different TES systems, which varied from 4 h–12h. General observations show that the increase in the TES system increases the annual energy production and capacity factor up to a specific limit. For this case, the technical components/parameters for the simulations are presented in Table 3. The results of the simulations are summarized in Table 8.

It can be observed in Table 8 that an increase in TES from 4 h to 12 h increased energy production and capacity factor. For cost assessment, it can be observed that LCOE reduced with an increase in the TES system. This result is attributed to the fact that a higher TES increased thermal energy and, consequently, energy production, which leads to a decrease in the LCOE. It is important to note that the results obtained in the present case are in agreement with the observations available in the literature [21]. Hence, the TES system 12 h will be considered in the present study for further simulations.

Table 7. Case 4: Results of simulations for a 50 MWe PT plant with different HTFs.

	HTF								
	Hitec Solar Salt	Caloria HT 43	Hitec XL	Therminol VP-1	Hitec	Dowtherm Q	Dowtherm RP	Therminol 59	Therminol 66
	Performance parameters								
Annual energy (GWh)	275.918	278.961	276.336	288.502	276.278	278.858	278.378	279.828	278.335
Gross-to-net conversion factor (%)	94.1	94.3	94.1	94.8	94.2	94.2	94.2	94.3	94.3
Capacity factor (%)	70	70.8	70.1	73.2	70.1	70.7	70.7	71	70.6
	Financial parameters								
Net capital cost (\$)	629,639,552	629,639,552	629,639,552	629,639,552	629,639,552	629,639,552	629,639,552	629,639,552	629,639,552
Nominal LCOE (¢/kWh)	3.63	3.59	3.63	3.48	3.63	3.6	3.6	3.58	3.6
Real LCOE (¢/kWh)	2.86	2.83	2.85	2.73	2.85	2.83	2.83	2.82	2.83

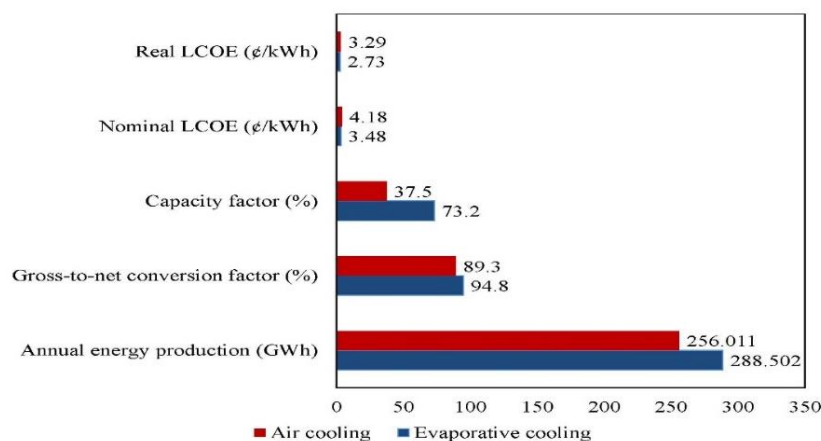
Table 8. Case 5: Results of simulations for a 50 MWe PT plant with different TES systems.

	TES		
	4	8	12
Performance parameters			
Annual energy (GWh)	191.185	245.833	288.502
Gross-to-net conversion factor (%)	94.7	94.8	94.8
Capacity factor (%)	48.5	62	73.2
Financial parameters			
Net capital cost (\$)	532,522,432	581,080,960	629,639,552
Nominal LCOE (¢/kWh)	4.5	3.79	3.48
Real LCOE (¢/kWh)	191.185	245.833	288.502

3.6. Case 6. A 50 MWe PT Plant with Different Types of Cooling Systems

In the sixth case, the performance and cost assessment of a 50 MWe PT plant were carried out using different types of cooling systems, including evaporative cooling and air cooling. The evaporative cooling (also known as wet cooling) is cheaper than the air cooling, and its efficiency is also higher. The water consumption in evaporative cooling is high (approximately 2100 L/MWh–3000 L/MWh), which requires a water source [21]. Unfortunately, there is a water resource scarcity in arid regions like the Middle East and North Africa (MENA) region, which discourages the use of evaporative cooling. However, the trend of using seawater as a cooling medium in evaporative cooling is increasing in the MENA region. This seawater can be used in a closed cycle and an open cycle. In an open cycle, the seawater leaving the condenser could be used for other processes, such as heating and desalination, whereas in a closed cycle, water is cooled down and recirculated. Conversely, air cooling (also known as dry cooling) is expensive and less efficient.

For this case, the technical components/parameters used for the simulations are presented in Table 3. The simulation results showed that the cooling water requirements of the proposed plant with evaporative and air cooling are 957,815 m³/year and 62,629 m³/year, respectively. Other simulation results are shown in Figure 8. It can be observed that evaporative cooling produced a higher amount of energy, a higher gross-to-net conversion, and a capacity factor with a lower LCOE. It is concluded that evaporative cooling is preferred for higher performance and lower LCOE.

**Figure 8.** Case 6: Results of simulations for a 50 MWe PT plant with different types of cooling. LCOE, levelized cost of energy.

3.7. Case 7. A 50 MWe PT Plant with Different Fossil Dispatch Mode

In the fossil dispatch mode, the PT plant is operated with a minimum backup level defined by the user. In this mode, the fossil fill fraction defines the fossil backup as a function of the thermal energy of the solar system (and storage, where applicable) at the given time and the total output of the designed

turbine. When the fossil fill fraction is greater than zero during the dispatch period in a minimum fossil backup level mode, the PT plant system is considered to contain a fossil burner, which heats the HTF before it is supplied to the power unit. For instance, if the fossil fill fraction is 1.0 for an hour, it means that if the solar energy delivered to the power cycle during that hour is less than the energy required to run the power unit at its gross output, the fossil fuel backup heater will supply the required energy to fulfill the demand. Similarly, if the fossil fill fraction is 0.25 for an hour, then the fossil fuel backup heaters would only supply the energy to the system when gross output drops below 25%.

For this case, the technical components/parameters for the simulations are presented in Table 3. Natural gas has been used as a backup fossil fuel because it is frequently used due to its low cost, low CO₂ emissions, and rapid response [31]. The results of the simulations are summarized in Table 9. In this case, it can be observed that with an increase in fossil fraction from 0.25 to 1.0, the performance of the PT plant increases in terms of annual energy, gross-to-net conversion, and capacity factor, while LCOE decreases. The highest annual energy (415.404 GWh), gross-to-net conversion (95.7%), and capacity factor (105.4%) are obtained with a fossil fill fraction of 1.0. Moreover, the lowest $LCOE_{(n)}$ (2.41 ¢/kWh) and $LCOE_{(r)}$ (1.9 ¢/kWh) are also obtained with fossil fill fraction 1.0. Therefore, it is concluded that a higher fossil fill fraction is preferred for higher performance and lower LCOE.

Table 9. Case 7: Results of simulations for a 50 MWe PT plant with different fossil dispatch modes.

	Fossil Fill Fraction			
	0.25	0.5	0.75	1
Performance parameters				
Annual energy (GWh)	320.304	349.953	382.775	415.404
Gross-to-net conversion factor (%)	94.6	95.2	95.5	95.7
Capacity factor (%)	81.3	88.8	97.1	105.4
Financial parameters				
Net capital cost (\$)	629,639,552	629,639,552	629,639,552	629,639,552
Nominal LCOE (¢/kWh)	3.13	2.87	2.62	2.41
Real LCOE (¢/kWh)	2.46	2.25	2.06	1.9

3.8. Case 8. A 50 MWe PT Plant with Suitable Parameter/Component

For the present case, the PT plant is operated with a suitable parameter/component obtained from the results of Cases 1–7, for performance improvement and cost reduction. Firstly, the effect of DNI on energy production has been investigated. The technical components/parameters for the simulations are presented in Table 3. The performance of a CSP plant is primarily dependent on the DNI. An increase or decrease in hourly DNI for the proposed location (as shown in Figure 6) leads to variation in the hourly power incident in the solar field and field thermal power produced, as demonstrated in Figure 9. It can be observed that with an increase or decrease in DNI (Figure 6), the power incident in the solar field and field thermal power produced increased or decreased. For instance, the lowest DNI was observed in December (Figure 6), which lead to the lowest power incident on the solar field (257.313 MWt) and the lowest field thermal power produced (107.74 MWt), while the highest DNI was observed in September (Figure 6), which lead to the highest power incident in the solar field (332.842 MWt) and the highest field thermal power produced (215.902 MWt). Further, the lowest monthly power incident in the solar field (1991.818 MWt) and the lowest monthly field thermal power (747.491 MWt) were observed in December, as depicted in Figure 10, whereas the highest monthly power incident on the solar field (2861.665 MWt) and highest monthly field thermal power (1887.211 MWt) were observed in June, as shown in Figure 10.

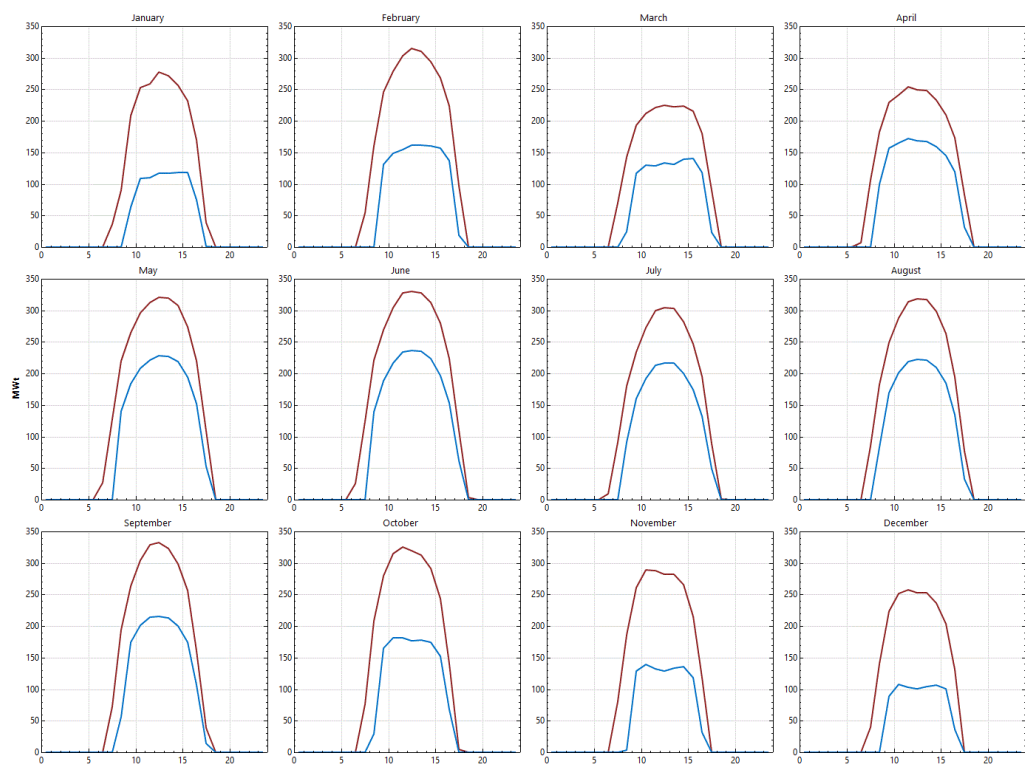


Figure 9. Hourly power incident in the solar field and field thermal power produced for Abu Dhabi, UAE.

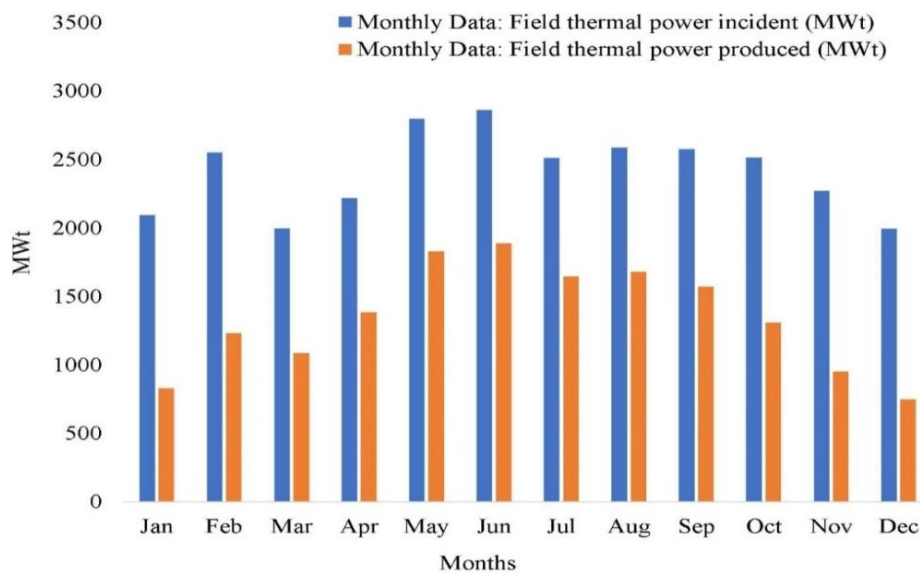


Figure 10. Monthly power incident in the solar field and field thermal power produced for Abu Dhabi, UAE.

Moreover, the monthly electricity production of the proposed PT plant is presented in Figure 11. As seen, the minimum and maximum monthly electricity production are obtained in February and December, respectively. Although the highest monthly power incident is observed in September, high electricity production is observed in July. Similarly, the lowest monthly power incident is observed in December, but the lowest electricity production is observed in February. The reason behind the phenomenon is the ambient temperature and the “cosine” effect.

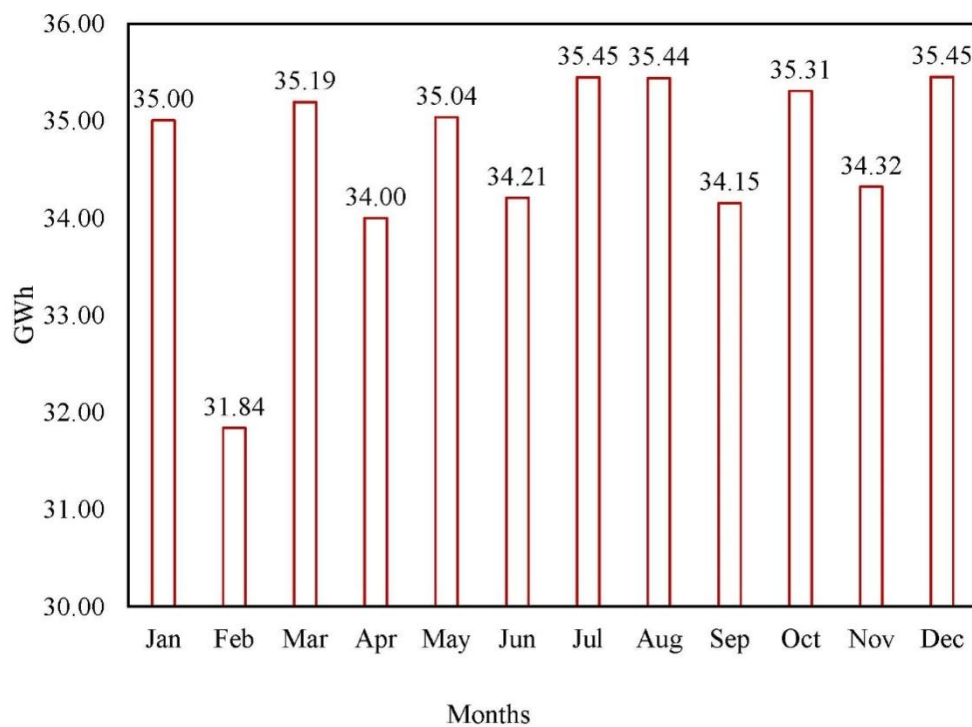


Figure 11. Monthly electricity production.

Other results obtained from the simulations are summarized in Table 10. In this case, it can be observed that the performance of the PT plant considerably increased in terms of annual energy, gross-to-net conversion, and capacity factor, whereas the LCOE dropped significantly. For instance, comparing case 8 with case1 ($SM = 4$), the energy production increased up to 52.69%, the gross-to-net conversion increased up to 2.93%, and the capacity factor increased up to 52.753%. On the other hand, $LCOE_{(n)}$ dropped up to 35%. It can be observed that the proper selection of parameters/components considerably improved the performance of the proposed PT plant and simultaneously reduced the energy cost. Therefore, the present study provides opportunities for decision-makers to choose the parameters and components for a CSP plant to enhance performance and reduce LCOE. It is worth noting that although the LCOE is low for the proposed study, it can be further reduced by considering the environmental and economic benefits of a CSP plant.

Table 10. Case 8: Results of simulations for a 50 MWe PT plant with suitable parameters/components. CDM, Clean Development Mechanism.

Description	Value
Performance parameters	
Annual energy (GWh)	415.404
Gross-to-net conversion factor (%)	95.7
Capacity factor (%)	105.4
Financial parameters	
Net capital cost (\$)	629,639,552
Nominal LCOE (¢/kWh)	2.41
Real LCOE (¢/kWh)	1.9
Nominal LCOE (¢/kWh) with CDM	2.35
Real LCOE (¢/kWh) with CDM	1.85

The CDM provides an opportunity for developed countries to invest in emission reduction projects for developing countries. This mechanism allows developed countries to acquire Certified Emissions Reductions (CER), which could help them achieve their emission reduction targets, set by the KP,

and provide economic benefits to the owner [32]. Since solar energy is environmentally friendly and its emissions of greenhouse gases (GHG) are negligible, solar energy projects, especially CSP plants, have received great attention for their use as aCDM [32]. Therefore, in this study, assessment of LCOE with CDMs was carried out. The baseline of the CSP project is kilowatt hours (kWh), produced by the CSP plant and multiplied by the emission coefficient (measured in kg CO₂e/kWh). It is assumed that the CSP plant has replaced a coal-fired power plant whose emissions are expected to be 980 g/kWh [20]. At present, the CER price is \$1/ton [33]. Based on the CDM, LCOE without and with CDM is presented in Figure 12. As expected, the internationalization of CO₂ emission reductions further reduces the nominal and real LCOE by the PT Plant. Moreover, the CSP plant without a fossil fill fraction reduced CO₂ emissions by up to 78,811,110 kg/year compared to the power plant operating with coal.

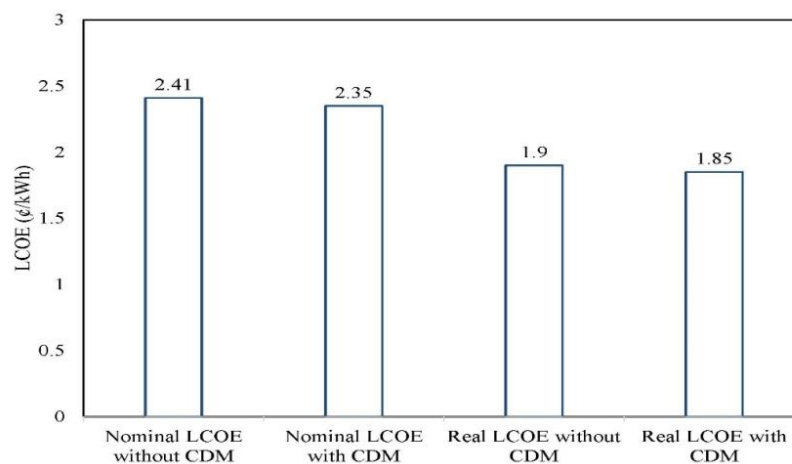


Figure 12. LCOE without and with a clean development mechanism (CDM).

The low LCOE revealed that CSP plants are economically viable. Therefore, it is concluded that the utilization of solar energy for CSP plants with a proper selection of technology can help reduce energy crises, eradicate environmental pollution, improve system performance, and reduce energy costs.

4. Conclusions

This paper presents the performance improvement and energy cost reduction of a 50MWePT plant for Abu Dhabi, UAE in the Middle-East region using the SAM software. The performance of a PT plant is greatly affected by the proper selection of technologies and components. A variety of technologies are commercially available and could be used in PT plants. In the present study, different technologies were incorporated for performance improvement and energy cost reduction. A total of eight cases were considered for the simulation of the proposed PT plant, including solar multiples, collectors, receivers, HTFs, cooling systems, TES systems, and fossil dispatch modes. Finally, simulations were carried out considering the best technologies/parameters. The key findings of the study are summarized as follows:

An increase in solar multiple increased energy production, the gross to net conversion factor, and the capacity factor but reduced the LCOE. The obtained optimum value for the solar multiple was 4. Further, an increase in the solar multiple slightly reduced the gross-to-net conversion factor, and the capacity factor while the LCOE increased.

For the collector/SCA, Luz LS-3 showed higher performance in terms of annual energy production and capacity factor, with the lowest LCOE. With different types of collectors/HCEs, differences in the results were minimal. Therefore, the SchottPTR70 2008 was selected because it is widely employed in PT plants worldwide.

In the case of simulations with different HTFs, the Therminol VP-1 achieved a higher annual energy production, gross-to-net conversion factor, and capacity factor. Conversely, the lowest LCOE

also corresponded to Therminol VP-1. The TES system varied from 4 h to 12 h to investigate the effects on the PT plant. An increase in TES increased the energy production and capacity factor and simultaneously reduced the LCOE. However, optimum TES was achieved at 12 h (TES = 12 h).

For analysis with different cooling systems (which include evaporative cooling and air-cooling), the results show that the performance of a PT plant with evaporative cooling was higher compared to a PT plant with air cooling. Since water scarcity is a significant issue in the MENA region, it was suggested to incorporate seawater as a cooling medium in the condenser instead of freshwater.

The performance of PT plants improved with the addition of a fossil fill dispatch from 0.25 to 1.0. Moreover, fossil fill fraction of 1.0 achieved the highest performance and lowest LCOE.

For the eighth case, which was found to be the best-case scenario in the study, simulations were carried out considering the most suitable results from the preceding seven cases. The effect of DNI on thermal power and electrical energy production were investigated. The proposed system produced 415.404 GWh with $LCOE_{(n)}$ 2.41 ¢/kWh. For the proposed case, the performance of the PT plant considerably increased in terms of annual energy, gross-to-net conversion, and capacity factor, whereas the LCOE dropped significantly. For instance, comparing case 8 with case 1 (SM = 4), the energy production increased up to 52.69%, the gross-to-net conversion increased up to 2.93%, and the capacity factor increased up to 52.753%. On the other hand, $LCOE_{(n)}$ dropped up to 35%. Moreover, when the economic benefit of a PT plant was considered, as per directions of the CDM of the KP, the nominal LCOE further reduced to 2.35 ¢/kWh.

Finally, it is concluded that utilizing solar energy for CSP plants, with a proper selection of technology, can help reduce energy crises, eradicate environmental pollution, improve system performance, and reduce energy costs. As such, this study provides some insight into CSP technologies that will help decision-makers to choose parameters and components for CSP plants to enhance performance and reduce the LCOE. The performance improvement and energy cost analysis of other CSP technologies, such as SPT and LFR, will be presented in our future works.

Author Contributions: All the authors contributed to this work. M.I.S., A.M., and Q.N.S. conceived and structured the study. M.I.S., S.A.U.R., S.A.S., and K.H. developed the model and analyzed the results and prepared the preliminary manuscript. M.I.S., A.M., S.A.U.R., and S.A.S. reviewed and finalized the manuscript.

Funding: This research received no external funding.

Acknowledgments: The authors highly acknowledge Mehran University of Engineering and Technology, SZAB Campus, Khairpur Mir's, Balochistan University of Engineering and Technology, Khuzdar, Mehran University of Engineering and Technology Jamshoro and, the University of Veterinary and Animal Sciences, Lahore for their support in completing this research work.

Conflicts of Interest: The authors declare no conflict of interest.

Appendix A

Table A1. Different commercially available collectors with specifications.

	Collectors								
	Euro Tough ET150	Luz LS-2	Luz LS-3	Solargenix SGX-1	Albiasa Trough AT150	Siemens Sunfield 6	SkyFuel SkyTrough (with 80 mm OD Receiver)	FLABEG Ultimate Trough RP6(with 89 mm OD Receiver for Oil HTF)	FLABEG Ultimate Trough RP6 (with 70 mm OD Receiver for Molten-Salt HTF)
Solar field area (acres)	249	284	247	284	248	249	243	183	190
Total land area (acres)	348	398	346	398	347	349	340	256	266
Reflective aperture area—m ²	817.5	235	545	470.3	817.5	545	656	1720	1720
Aperture width-total structure—m	5.75	5	5.75	5	5.7	5.77	6	7.53	7.53
Length of collector assembly—m	150	49	100	100	150	95.2	115	247	247
Number of modules per assembly	12	6	12	12	12	8	8	10	10
Length of a single module—m	12.5	8.16	8.33	8.33	12.5	11.9	14.37	24.7	24.7

Appendix B

Table A2. Different commercially available receivers with specifications.

	Receivers							
	Schott PTR70	Schott PTR70 2008	Solel UVAC 3	Siemens UVAC 2010	Schott PTR80	Royal Tech CSP RTUVR 2014 (Manufacturer Specifications)	Royal Tech CSP RTUVR 70M4 (Manufacturer Specifications)	TRX70-125 (Manufacturer Specifications)
Absorber tube inner dia—m	0.076	0.066	0.066	0.066	0.076	0.066	0.066	0.066
Absorber tube outer dia—m	0.08	0.07	0.07	0.07	0.08	0.07	0.07	0.07
Glass envelope inner dia—m	0.115	0.115	0.115	0.109	0.115	0.119	0.1196	0.119
Glass envelope outer dia—m	0.12	0.12	0.121	0.115	0.12	0.125	0.125	0.125
Absorber flow pattern	Tube flow	Tube flow	Tube flow	Tube flow	Tube flow	Tube flow	Tube flow	Tube flow
Absorber material type	304L	304L	304L	216L	304L	321H	321H	321H

Appendix C

Table A3. Different commercially available HTFs with specifications.

	HTF								
	Hitec Solar Salt	Caloria HT 43	Hitec XL	Therminol VP-1	Hitec	Dowtherm Q	Dowtherm RP	Therminol 59	Therminol 66
Storage Volume—m ³									
TES Thermal capacity—MWht	1589	1589	1589	1589	1589	1589	1589	1589	1589
Tank diameter—m	36	45	37	45	36	45.1	43.42	44.3081	42.6
Min fluid volume—m ³	1038	1601	1078	1609	1059	1598	1481	1541	1429
Est. heat loss	0.4	0.57	0.43	0.57	0.433	0.966	0.54	0.55	0.52
Thermal storage exergetic efficiency	1	0.96	0.96	0.966	0.966	0.966	0.966	0.966	0.966
Storage HTF min T (°C)	238	−12	120	12	142	−35	0	−45	0
Storage HTF max T (°C)	593	315	500	400	538	330	330	315	345
TES fluid density—kg/m ³	1872	643.9	1957	765	1829	721	791.72	715	780
TES Specific heat—kJ/kg-k	1.5	2.93	1.4	2.45	1.56	2.6	2.57	2.7	2.7

References

- Behar, O.; Khellaf, A.; Mohammedi, K. A review of studies on central receiver solar thermal power plants. *Renew. Sustain. Energy Rev.* **2013**, *23*, 12–39. [[CrossRef](#)]
- Hussain, N. *Development of Energy Modeling And Decision Support Framework for Sustainable Electricity System of Pakistan*; Mehran University of Eng. Technology: Jamshoro, Pakistan, 2019.
- Fuqiang, W.; Ziming, C.; Jianyu, T.; Yuan, Y.; Yong, S.; Linhua, L. Progress in concentrated solar power technology with parabolic trough collector system: A comprehensive review. *Renew. Sustain. Energy Rev.* **2017**, *79*, 1314–1328. [[CrossRef](#)]
- Ummadisingu, A.; Soni, M.S. Concentrating solar power—Technology, potential, and policy in India. *Renew. Sustain. Energy Rev.* **2011**, *15*, 5169–5175. [[CrossRef](#)]
- Solangi, Y.A.; Tan, Q.; Mirjat, N.H.; Valasai, G.D.; Khan, M.W.A.; Ikram, M. An Integrated Delphi-AHP and Fuzzy TOPSIS Approach toward Ranking and Selection of Renewable Energy Resources in Pakistan. *Processes* **2019**, *7*, 118. [[CrossRef](#)]
- REN21. Renewable Global Status Report. REN21 Secretariat, Paris. 2016. Available online: <http://www.ren21.net/status-of-renewables/global-status-report/> (accessed on 20 January 2017).
- Solangi, K.H.; Islam, M.R.; Saidur, R.; Rahim, N.A.; Fayaz, H. A review on global solar energy policy. *Renew. Sustain. Energy Rev.* **2011**, *15*, 2149–2163. [[CrossRef](#)]
- Mengal, A.; Mirjat, N.H.; Walasai, G.D.; Khatri, S.A.; Harijan, K.; Uqaili, M.A. Modeling of Future Electricity Generation and Emissions Assessment for Pakistan. *Processes* **2019**, *7*, 212. [[CrossRef](#)]
- Calif, R.; Schmitt, F.G.; Huang, Y.; Soubdhan, T. Intermittency study of high frequency global solar radiation sequences under a tropical climate. *Sol. Energy* **2013**, *98*, 349–365. [[CrossRef](#)]
- Calif, R.; Schmitt, F.G.; Medina, O.D. -5/3 Kolmogorov turbulent behavior and Intermittent Sustainable Energies. In *Sustainable Energy*; Zobia, A., Aleem, S.A., Afifi, S.N., Eds.; Intech: London, UK, 2016.
- Sharma, C.; Sharma, A.K.; Mullick, S.C.; Kandpal, T.C. Cost reduction potential of parabolic trough based concentrating solar power plants in India. *Energy Sustain. Dev.* **2018**, *42*, 121–128. [[CrossRef](#)]
- Haneklaus, N.; Zheng, Y.; Allelein, J.H. Stop Smoking—Tube-In-Tube Helical System for Flameless Calcination of Minerals. *Processes* **2017**, *5*, 67. [[CrossRef](#)]
- Peterseim, J.H.; White, S.; Tadros, A.; Hellwig, U. Concentrated solar power hybrid plants, which technologies are best suited for hybridisation? *Renew. Energy* **2013**, *57*, 520–532. [[CrossRef](#)]
- IEA (International Energy Agency). *Solar Energy Perspectives*; IEA (International Energy Agency): Paris, France, 2011.
- IRENA. *Renewable Energy Technologies: Cost Analysis Series; Working Paper on Power Sector—Concentrating Solar Power, Vol.1, 2/5*; International Renewable Energy Agency (IRENA): Abu Dhabi, United Arab Emirates, 2012.
- Zhang, H.L.; Baeyens, J.; Degreève, J.; Cacères, G. Concentrated solar power plants: Review and design methodology. *Renew. Sustain. Energy Rev.* **2013**, *22*, 466–481. [[CrossRef](#)]
- Soomro, M.I.; Kim, W.-S. Performance and economic evaluation of linear Fresnel reflector plant integrated direct contact membrane distillation system. *Renew. Energy* **2018**, *129*, 561–569. [[CrossRef](#)]
- Kearney, D.; Herrmann, U.; Nava, P.; Kelly, B.; Mahoney, R.; Pacheco, J.; Cable, R.; Potrovitza, N.; Blake, D.; Price, H. Assessment of a molten salt heat transfer fluid in a parabolic trough solar field. *J. Sol. Energy Eng.* **2003**, *125*, 170–176. [[CrossRef](#)]
- Giostrì, A.; Binotti, M.; Astolfi, M.; Silva, P.; Macchi, E.; Manzolini, G. Comparison of different solar plants based on parabolic trough technology. *Sol. Energy* **2012**, *86*, 1208–1221. [[CrossRef](#)]
- Wagner, S.J.; Rubin, E.S. Economic implications of thermal energy storage for concentrated solar thermal power. *Renew. Energy* **2014**, *61*, 81–95. [[CrossRef](#)]
- Kassem, A.; Al-Haddad, K.; Komljenovic, D. Concentrated solar thermal power in Saudi Arabia: Definition and simulation of alternative scenarios. *Renew. Sustain. Energy Rev.* **2017**, *80*, 75–91. [[CrossRef](#)]
- Liu, M.; Tay, N.H.S.; Bell, S.; Belusko, M.; Jacob, R.; Will, G.; Saman, W.; Bruno, F. Review on concentrating solar power plants and new developments in high temperature thermal energy storage technologies. *Renew. Sustain. Energy Rev.* **2016**, *53*, 1411–1432. [[CrossRef](#)]
- System Advisor Model (SAM). National Renewable Energy Laboratory. Available online: <https://sam.nrel.gov/> (accessed on 16 November 2018).

24. Purohit, I.; Purohit, P.; Shekhar, S. Evaluating the potential of concentrating solar power generation in Northwestern India. *Energy Policy* **2013**, *62*, 157–175. [[CrossRef](#)]
25. SOLARGIS. Available online: <https://solargis.com/maps-and-gis-data/download/united-arab-emirates> (accessed on 13 March 2018).
26. Goebel, O. Shams one 100 MW CSP plant in Abu Dhabi. Update on projects status. In Proceedings of the 17th SolarPaces Conference, Granda, Spain, 20–23 September 2011.
27. System Advisor Model (SAM). National Renewable Energy Laboratory. Available online: <https://sam.nrel.gov/weather> (accessed on 20 November 2018).
28. System Advisor Model (SAM). National Renewable Energy Laboratory. Available online: <https://sam.nrel.gov/financial> (accessed on 22 November 2018).
29. Guzman, L.; Henao, A.; Vasquez, R. Simulation and Optimization of a Parabolic Trough Solar Power Plant in the City of Barranquilla by Using System Advisor Model (SAM). *Energy Procedia* **2014**, *57*, 497–506. [[CrossRef](#)]
30. NREL: Concentrating Solar Power Projects. Available online: <http://www.nrel.gov/csp/solarpaces/> (accessed on 1 March 2018).
31. Miguel, G.S.; Corona, B. Hybridizing concentrated solar power (CSP) with biogas and biomethane as an alternative to natural gas: Analysis of environmental performance using LCA. *Renew. Energy* **2014**, *66*, 580–587. [[CrossRef](#)]
32. Purohit, I.; Purohit, P. Techno-economic evaluation of concentrating solar power generation in India. *Energy Policy* **2010**, *38*, 3015–3029. [[CrossRef](#)]
33. United Nations Framework Convention on Climate Change. Available online: <https://offset.climateneutralnow.org/allprojects?ProjectNumber> (accessed on 9 October 2017).



© 2019 by the authors. Licensee MDPI, Basel, Switzerland. This article is an open access article distributed under the terms and conditions of the Creative Commons Attribution (CC BY) license (<http://creativecommons.org/licenses/by/4.0/>).